Density-based Compressible Solver with Equilibrium Cavitation Model in OpenFOAM

Mohammad Hossein Arabnejad[*], Rickard Bensow[*],Claes Eskilsson[*]
[*]Department of Shipping and Marine Technology, Chalmers University of Technology, Gothenburg, Sweden
mohammad.h.arabnejad@chalmers.se

1 Introduction

Cavitation is responsible for vibration, erosion and performance degradation in many engineering devices. To better understand cavitation and avoid its undesirable effects, cavitating flows have been the subject of many numerical studies. In most of these studies, the simulation is based on a two-phase incompressible Navier-Stokes solver together with a mass-transfer model. Because of their incompressible assumption, these solvers are not able to capture shock waves and high pressure peaks which are essential in the physics of cavitation erosion. Furthermore, the mass-transfer models normally include several empirical parameters. These parameters must be tuned for a particular flow condition and geometry by several numerical experiments.

An alternative approach to two-phase incompressible solvers is to use density-based compressible solvers with equilibrium cavitation models. These cavitation models assume that the two phases are in thermal and mechanical equilibrium and the transition between phases can be modeled by an equation of state for the mixture density. A widely used example of equilibrium cavitation models is the barotropic cavitation model (Venkateswaran et al.,2002). In this model, the densities of the fluids are assumed to depend only on pressure. With the barotropic assumption, the pressure gradient is always aligned with the density gradient, therefore the barotropic term in vorticity transport equation becomes zero. Gopalan and Katz (2000) have shown that the barotropic vorticity generation is important in closure region of sheet cavities. The under-prediction of the barotropic vorticity term can be avoided by using a more complete equilibrium cavitation model introduced by Saurel et al. (2002). In this approach, the full set of equations, including the energy equation, are solved with the suitable temperature dependent equations of state for each phase. This approach has been successfully used for different cavtiating flows by Koop (2008) and Schnerr et al. (2008).

The purpose of this paper is to present an implementation of a density-based compressible solver with equilibrium cavitation (similar to Koop (2008) and Eskilsson and Bensow (2012)) in the open-source finite volume framework OpenFOAM (Jasak et al.,1995). To check the implementation, simulation of a 1D Riemann water problem and a collapsing bubble are considered. Then, the validated solver is used to simulate the cavitating flow over a 2D NACA0015 foil.

2 Governing Equations

In the present study, the compressible Euler equations are used as the governing equations. These equations include continuity, momentum, and energy equations. To close the governing equations, an equation of state (EOS) is required to provide the relations between pressure and temperature with internal energy and density. In two-phase water-vapour flows, three equations of states must be provided for the three possible cases.

Pure Liquid

If the calculated density is higher than the liquid saturation density, the fluid is assumed to be pure liquid. The liquid phase is then described by the modified Tait EOS (Saurel et al., 1999),

$$p(\rho,T) = K_0\left[\left(\frac{\rho}{\rho_{l,sat}(T)}\right)^N - 1\right] + p_{sat}(T). \quad (1)$$

The temperature is obtained by the caloric EOS,

$$T = \frac{e-e_{l0}}{C_{vl}} + T_0. \quad (2)$$

Pure Vapour

When the density drops below the vapour saturation density, the fluid is assumed to be pure vapour. The perfect gas law is used to describe the pure vapour phase,

$$p(\rho,T) = \rho RT. \quad (3)$$

The temperature is obtained by the caloric EOS,

$$T = \frac{e-e_{l0}-L_v(T_0)}{C_{vv}} + T_0. \quad (4)$$

Mixture phase

With the thermodynamic equilibrium assumption, the mixture pressure can be considered equal to saturation pressure,$p = p_{sat}(T)$. The temperature is calculated from the equation of internal energy in the mixture as,

$$T = \frac{\rho(e-e_{l0})-\alpha\rho_{v,sat}L_v(T_0)}{\alpha\rho_{v,sat}C_{vv}+(1-\alpha)\rho_{l,sat}C_{vl}} + T_0, \quad (5)$$

where α is the vapour fraction and can be computed from the mixture density,

$$\alpha = \frac{\rho-\rho_{l,sat}}{\rho_{v,sat}-\rho_{l,sat}}. \quad (6)$$

The parameters in above equations are given in Table 1. The saturated values of pressure, $p_{sat}(T)$, and liquid and vapour density, $\rho_{l,sat}$ and $\rho_{v,sat}$, used in the above equations are obtained from IAPWS-IF97 library(Wagner et al. ,2008).

Table 1: Parameters used in Eq.1-6

N	K_0	C_{vl} $(Jkg^{-1}K^{-1})$	T_0 (K)	e_{l0} (Jkg^{-1})	γ	R $(Jkg^{-1}K^{-1})$	C_{vl} $(Jkg^{-1}K^{-1})$	$L_v(T_0)$ $(Jkg^{-1}K^{-1})$
7.15	3.3×10^8	4180	1.0×10^4	617.0	1.327	461.6	1410.8	2.753×10^6

3 Numerical Methods

The following numerical method has been implemented in OpenFOAM. The numerical flux is evaluated by solving the approximate Riemann problem using HLLC-AUSM low-Mach Riemann solver (Koop,2008). Second order accuracy in space is achieved by the piece-wise linear

reconstruction method with the limiter function of Venkatakrishnan (1995). For time advancing, explicit low storage Runge-Kutta schemes are employed.

4 Results

4.1 Validation

In order to validate the implementation of the compressible solver, numerical simulations of a 1D Riemann problem for water flow and a collapsing bubble are performed.

1D Riemann problem for water flow

In this section, the simulation of 1D Riemann problem for water flow is presented. The purpose of this simulation is to check the capability of the implemented method in capturing shock waves in compressible water flows. The computational domain, shown in Fig. 1, is a tube of length 1m filled with water. A diaphragm at the center of the tube separates two regions with different initial conditions. This diaphragm is removed at the start of simulation.

The solution of this Riemann problem includes a left-running expansion wave, a contact surface, and a right-running shockwave. The numerical solution at different instances is plotted in Fig. 2, which shows that the implemented numerical methods are able to capture expansion and shock waves without overshoot.

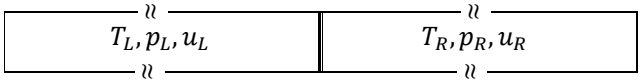

p_L (pa)	u_L (m/s)	T_L (K)	p_R (pa)	u_R (m/s)	T_R (K)
1.0×10^8	0.0	293	$1e \times 10^4$	0.0	293

Fig. 1: Computational domain and initial conditions for 1D Riemann problem for water flow

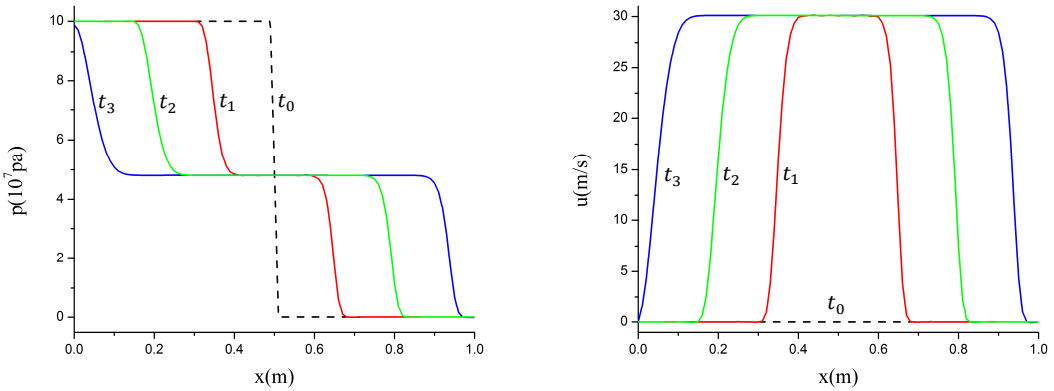

Fig. 2: Solution of Riemann problem for water flow at $t_N = N\Delta t$ (left: pressure, right: velocity, $\Delta t = 9 \times 10^{-5}$).

Collapsing Bubble

In this section, the implementation of a homogeneous cavitation model is validated for the collapse of a single bubble. To minimize the computational cost, an asymmetric wedge mesh with angle of five degrees is created. The mesh is a section of a sphere and has 100 cells in radial direction and 100 cells in circumferential direction. The mesh spacing is very refined near the location of bubble collapse in order to capture the rapid movement of bubble interface. The computational domain and boundary conditions are shown in Fig. 3. As the initial conditions, the pressure inside the bubble is set to $P_v = 2340\ pa$,while the pressure in surrounding liquid is $P_\infty = 1bar$.

To compare numerical results with the solution of the Rayleigh-Plesset equation, this equation is solved using the ODE solver in OpenFOAM. The fluid properties that are used in this solution are the same as those in numerical simulation. Fig. 4 shows the agreement between the result of numerical simulation and the solution of Rayleigh-Plesset equation. This agreement demonstrates the validation of the implemented cavitation model and numerical methods.

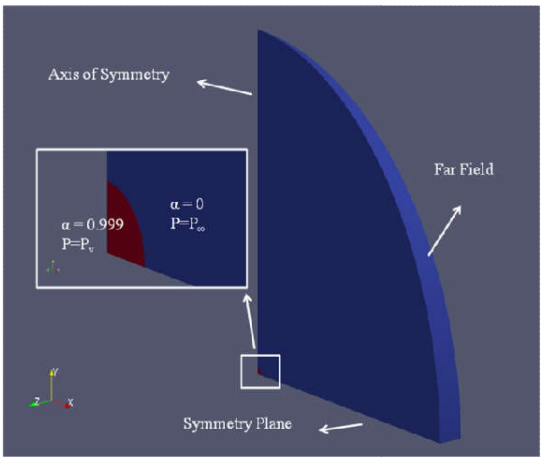

Fig. 3: Computational Domain and BCs for the collapsing bubble case.

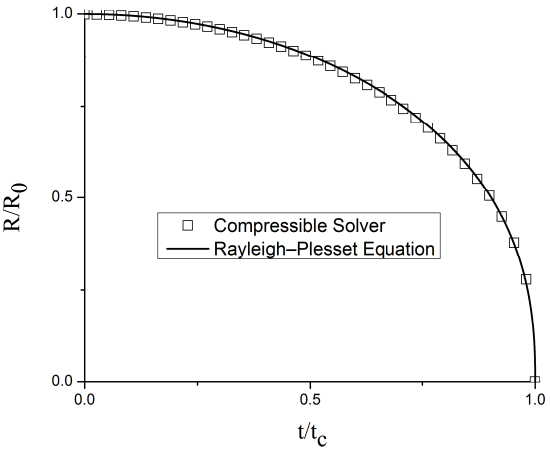

Fig. 4: Comparison of numerical simulation and solution of Rayleigh-Plesset equation for a collapsing bubble.

4.2 Cavitating Flow over 2D NACA0015

The hydrofoil considered in this study, is a 2D NACA0015 foil at an angle of attack of 6^o with chord length c = 0.13m. The computational domain, shown in Fig. 5, is a channel with height 2c and a length of 2c upstream of the hydrofoil leading edge and 3c behind the trailing edge. The inlet velocity is 12 m/s, the temperature 293 k and the density 998.2 kg/m^3. The pressure at the outlet is set to 74.2 kPa which corresponds to the cavitation number equal to one. Slip boundary conditions are applied to the foil and the channel walls, as the Euler flow is computed. A C-type mesh with 38280 cells is used for this simulation.

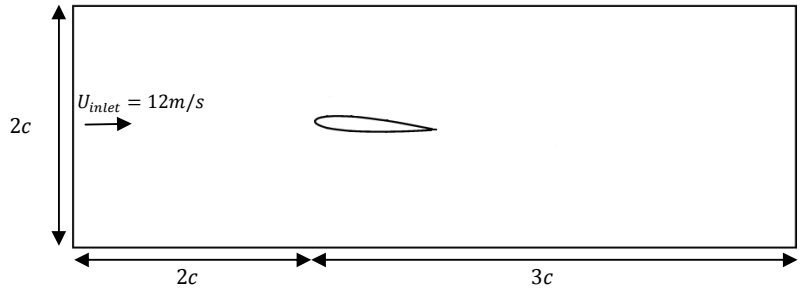

Fig. 5: Computational domain for simulation of cavitating flow over 2D NACA0015.

Koop (2008) has reported that for this case, the growth and shedding of the sheet cavity has an approximately periodic behavior. To show this behavior, the total vapour volume V_{vap} is calculated at every time step. The time history of the total vapor volume V_{vap} during several cycles are presented in Fig. 6. The figure shows a periodic behavior with period of 0.025s and a frequency of 40 Hz.

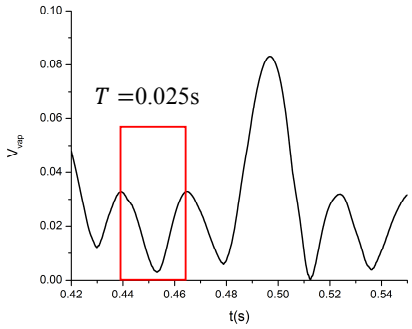

Fig. 6: Time-history of the total vapor volume V_{vap} in simulation of the cavitating flow over 2D NACA0015

In Fig. 7, the distribution of vapour fraction α is presented for a number of equidistant time instances during one cycle. At the start of the cycle, Fig7.(a), a new sheet cavity appears at the leading edge, while the shed cloud cavity from previous cycle is convected downstream. The sheet cavity continues to grow and the shed vapour structure starts collapsing as it is transported into the high pressure region near the trailing edge ,Fig.7(b). The collapse of the shed vapour structure produces a high pressure pulse which is shown in Fig 8(a). As the sheet cavity has reached its maximum length, a re-entrant jet has developed at the closure region of the sheet cavity, Fig.7(c). The re-entrant jet travels upstream along the foil surface and collides with the liquid interface. This collision splits the sheet cavity into several vapour structures with rotational motion, Fig.7(d-e). While the shed vapour structures merge by circular motion and create a cloud cavity, Fig.7(f), the remaining part of sheet cavity collapses leading a pressure pulse shown in Fig 8(b).

5 Conclusion

A density based compressible solver with equilibrium cavitation model has been implemented in OpenFOAM. The implemented solver is tested for three cases. The simulation of 1D Riemann problem for water flow and collapsing bubble are performed to validate the implemented numerical methods and cavitation model. After checking the implementation, the simulation of a cavitiating flow

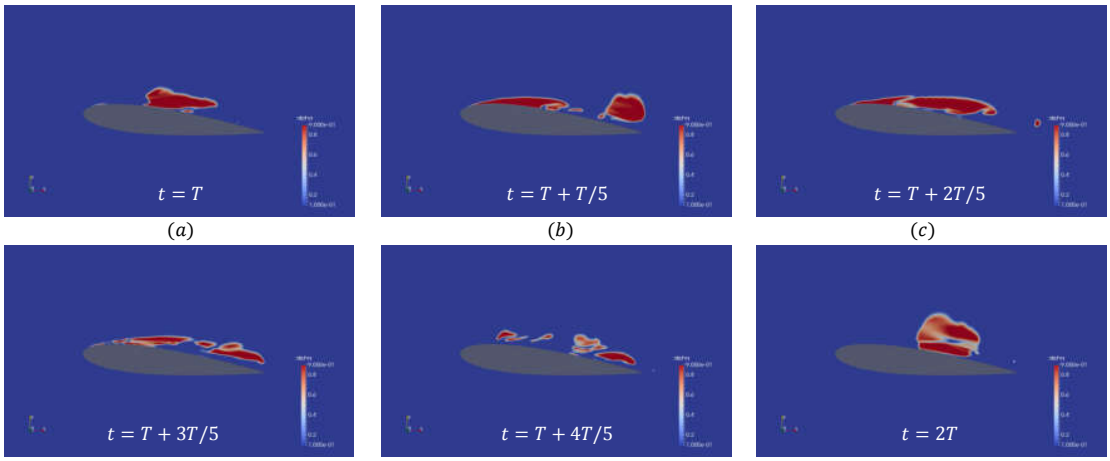

(a) (b) (c) (d) (e) (f)

Fig. 7: Distribution of vapour fraction α during one shedding cycle.

(a) (b)

Fig. 8:Pressure pulses produced by the collapse of (a)the cloud cavity and (b)the sheet cavity.

over a 2D NACA0015 foil is performed. The results show that the cavitating flow has a periodic behavior with the frequency of 40 Hz. The re-entrant jet mechanism is found to be responsible for this periodic behavior. In the future, the solver will be extended to include viscous fluxes. Furthermore, the solver will be used to simulation cavitating flows in 3D and compare with experimental data.

References

C. Eskilsson ,R. Bensow(2011). A compressible model for cavitating flow: comparison between Euler, RANS and LES simulations. 29th Symposium on Naval Hydrodynamics, Gothenburg, Sweden.

S. Gopalan and J. Katz(2000). Flow structure and modeling issues in the closure region of attached cavitation, *Physics of Fluids*, **12**(4), 895–911.

H. Jasak H.G. Weller, G. Tabor and C. Fureby(1998). A tensorial approach to CFD using object oriented techniques. *Computer in Physics*, **12**(6).

A.H. Koop (2008), Numerical Simulation of Unsteady Three Dimensional Sheet Cavitation, PhD thesis, University of Twente.

R. Saurel, and R. Abgrall(1999). A multiphase Godunov method for compressible multifluid and multiphase flow, *Journal of Computational Physics*,**150**, 425–467.

G.H. Schnerr, I.H. Sezal, and S.J. Schmidt (2008) Numerical investigation of three-dimensional cloud cavitation with special emphasis on collapse induced shock dynamics. *Physics of Fluids*, **20**, 40703.

W. Wagner and H. Kretzschmar (2008). *International steam tables: properties of water and steam, based on the industrial formulation IAPWS-IF97*. Springer.

V. Venkatakrishnan(1995). Convergence to Steady-State Solutions of the Euler Equations on Unstructured Grids with Limiters". *Journal of Computational Physics*, **118**,120–130.

S. Venkateswaran, J.W. Lindau, R.F. Kunz, and C.L. Merkle (2002) Computation of multiphase mixture flows with compressibility effects, *Journal of Computational Physics*, **180**, 54–77.